

Geochemistry and Petrogenetic Affinity of the Rocks of Pella and Environs, Hawal Massif Northeast Nigeria

Kwache, J.B.

Regional Geology Department, Nigerian Geological Survey Agency, Utako District, Abuja, Nigeria.

Corresponding E-mail: jbkwache@gmail.com

Abstract

Pella and environs is situated on Hawal Massif of northeastern Basement Complex of Nigeria. It covers an area of about 216.8km². The rocks in the area has for long been described as undifferentiated Basement Complex. This paper is aimed at differentiating and suggesting the petrogenetic affinity of the rocks by combing field data with petrography and geochemistry. Stream, compass and road traversing were employed to geologically map outcropping components. Petrographic studies of four thin sections were studied using Steindorff Mel Sobel Petrological Microscope. Atomic Absorption Spectrometry (AAS) method was employed to analyze eighteen pulverized samples. The geochemical results were interpreted using PetroGraph version 2 beta software. These results differentiated the rocks into migmatite-gneiss, granite gneiss, Older Granites and basalts. Major mineral modes in migmatite-gneiss, granite gneiss and the Older granites are quartz, feldspars and biotite while basalt is dominated by plagioclase, olivine and sanidine. Migmatite-gneiss, granite gneiss and the Older Granites have similarities of geochemical data with enrichment in SiO₂, ranging from 67.52 - 71.02 wt. %, K₂O ranges from 3.35 - 4.40 wt. % and Na₂O ranges from 1.87 - 4.00 wt. %. Basalts are enriched in MgO with ranges from 5.99 - 6.78 wt. %, TiO₂ ranges from 3.27 - 4.35 wt. %, Fe₂O₃ ranges from 14.1 - 15.5 wt. % and CaO ranges from 7.11 - 7.64 wt. %. Pegmatite are enriched in K₂O with ranges from 9.98 - 11.4 wt. % but depleted in CaO with ranges from 0.40 - 0.76 wt. % and TiO₂ from 0.06 - 0.12 wt. %. Some selected oxides and trace elements plotted on Harker using SiO₂ for gneisses, granites and pegmatite and MgO for basalts as fractionation index revealed that Fe₂O₃, CaO, Co, Sr, Al₂O₃ and K₂O shows a continuous negatively correlated well-defined linear trend. The chondrite-normalized Rare Earth Elements (REE) patterns of most of the rocks are characterized by enrichment in Light Rare Earth Elements (LREE) relative to depletion in Heavy Rare Earth Elements (HREE). The negative anomalies shown by Eu are prominent in the rocks. Total-Alkaline-Silica (TAS) discrimination plot of SiO₂ vs. Na₂O + K₂O revealed that granite gneiss and granite falls within granitic field. Alumina-Iron-Magnesium (AFM) diagrams for gneisses, granites and pegmatite revealed Calc-alkaline while basalt is tholeiitic. Discrimination plots of Rb vs. (Yb + Ta) for granite gneiss and granites revealed Syn-Collision (Syn-COLG) and Volcanic Arc Granite (VAG). The granites are I-type, metaluminous to weakly peraluminous and have continental crust affinity. Basalts are Mid Oceanic Ridge (MORB) with mantle affinity. All the rocks suggest fractionation and igneous progenitor.

Keywords: Pella, undifferentiated, differentiated, Calc-alkaline, tholeiitic, fractionation, enrichment, affinity, progenitor

Introduction

Little is known about the geology of the northeastern Basement Complex of Nigeria and thus for long has been described as undifferentiated Basement Complex (McCurry 1976). However, Adekeye and Ntekim (2004), Patrick (2005), Bassey (2006), Bassey, N. E. and Valdon, Y.B. (2011) and Kwache and Ntekim (2015) worked in Song and environs of the northeastern Basement Complex and reported that migmatites, gneisses and Older Granites are the dominant rock units in the area. These authors submitted that the granites consist mostly of medium to coarse grained and coarse grained to porphyritic varieties with well-developed sub-hedral to euhedral crystals which have experienced extensive faulting and shearing. According to them, migmatites and the gneisses are extensively intruded by granitic rocks of the Pan African Orogeny (600 ± 150ma). They further reported that the granites are commonly intruded by pegmatite and basalts with the basalts occurring as extensive flows and unconformably

overlying the basement rocks. Pella and environs form part of the northeastern Basement Complex. This paper therefore combines field data with petrography, major, trace and rare earth elements data to differentiate and suggest the petrogenetic affinity of the rocks of Pella and Environs.

Study Location

Pella and environs is situated on the eastern part of Hawal Massif of the northeastern Basement Complex of Nigeria (Figure 1A). Hawal Massif is bounded by the Tertiary - Quaternary Chad Basin to the north, the Yola and Gongola arms of the Cretaceous Benue Trough to the west and south and the Cameroun mountains to the east. The study area consists of high and low topography (Figures 1A and 1B). It lies within geographical coordinates; latitudes 10°07'N and 10°15'N and Longitudes 12°45'E and 13°00'E. It covers an area of about 216.8 km² and is accessible by both major and minor roads.

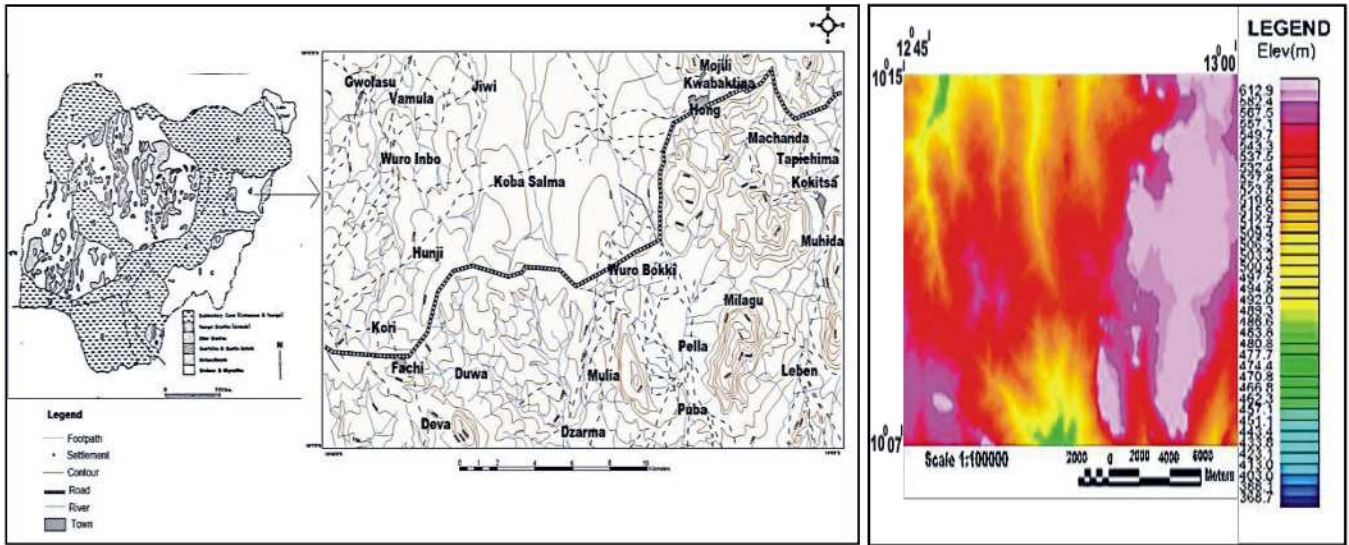


Fig. 1a: Topographic map of Pella and environs Figure 1B. SRTM Imagery of Pella and environs (Federal Surveys, 1968)

Materials and Methods

Materials used include but not limited to hammers, GPS, compass, hand lens, etc. PetroGraph version 2 beta, GeoRose and Microsoft statistical software were used for geochemical interpretations and joint directions respectively. Steindorff Mel Sobel Petrological Microscope was also used for petrographic studies. Stream, compass and road traversing were employed to geologically map outcropping components in the study area. A total of forty rock samples were collected out of which four representative samples were selected for petrographic and eighteen samples were equally selected for geochemical analysis from different lithologic units. Petrographic studies were carried out at the Nigerian Geological Survey Agency mini petrological laboratory in Abuja. Geochemical analyses of major, trace and rare earth elements were carried out ACME Lab in Canada using Atomic Absorption Spectrometry (AAS).

Results

Lithologic Units

Ground truthing revealed that Pella and environs is underlain by the Pre-Cambrian Basement Complex rocks. The major (mappable) rock units in the area are migmatite-gneiss (Figure 2), medium grained granite (Figure 3) and coarse porphyritic granite (Figure 4). Minor (unmappable) rocks are granite gneiss, coarse grained granite, pegmatite and basalts (Figure 5) with subordinate veins of quartz and aplite. The geologic map is presented in Figure 6.



Fig. 2: Migmatite-Gneiss



Fig. 3: Medium Grained Granite



Fig. 4: Coarse Porphyritic Granite



Fig. 5: Basalt

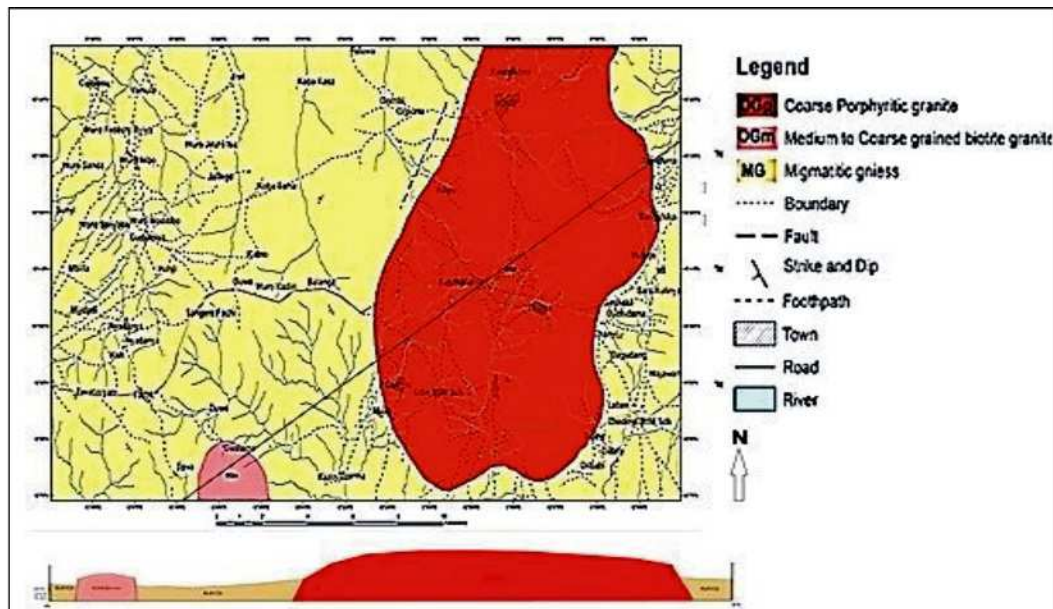


Fig. 6: Geologic map of Pella and Environs

Petrography

Migmatite-gneiss, medium grained granite, coarse porphyritic granite and basalt were studied. The mineral modes in migmatite-gneiss are hornblende, plagioclase, orthoclase, biotite, zircon, pyroxene, opaque and quartz (Figure 7A and 7B). The medium grained granite consists of quartz and has other minerals such as muscovite, hornblende, plagioclase, orthoclase, microcline, biotite, zircon and opaque (Figures 8A and 8B). Coarse porphyritic granite which is dominated by microcline feldspar also consists of muscovite, hornblende, plagioclase, orthoclase, quartz, biotite, sphene and opaque minerals (Figures 9A and 9B). The mineral assemblages in basalt which is dominated by plagioclase include, sanidine, pyroxene, quartz, olivine, hornblende and opaque (Figure 10A and 10B).

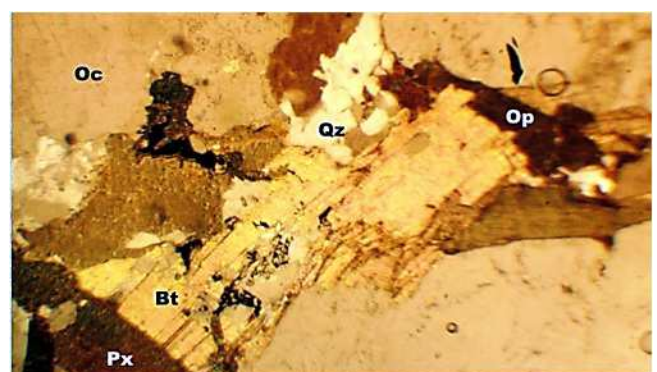


Fig. 7a: Photomicrograph of migmatite gneiss

Geochemistry

Geochemical result is presented in Table 1. Migmatite-gneiss is represented by MG, granite gneiss (GG),

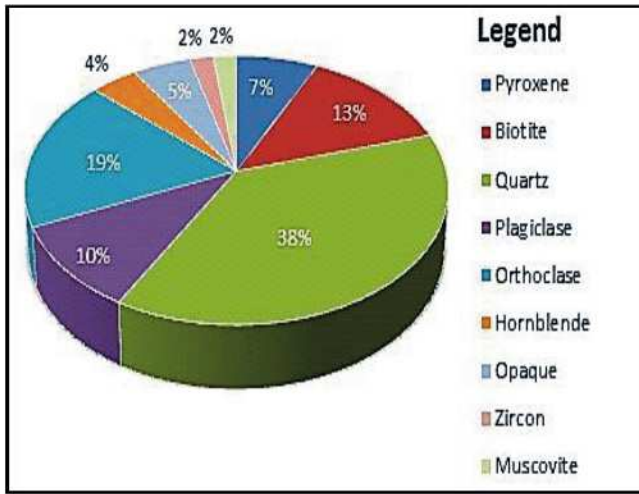


Fig. 7b: Modal composition of migmatite gneiss under cross polar (x20)

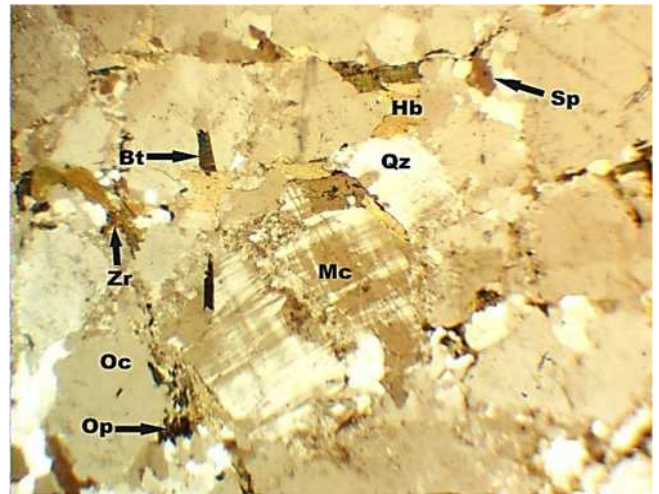


Fig. 9a: Photomicrograph of coarse porphyritic polar (x20)

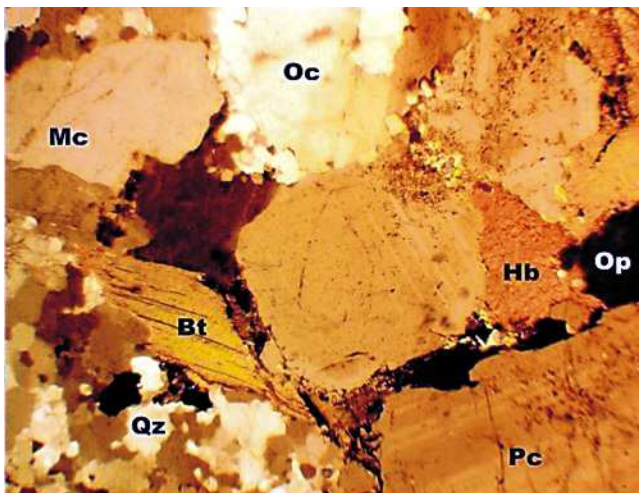


Fig. 8a: Photomicrograph of medium grained under cross polar (x20) grained granite

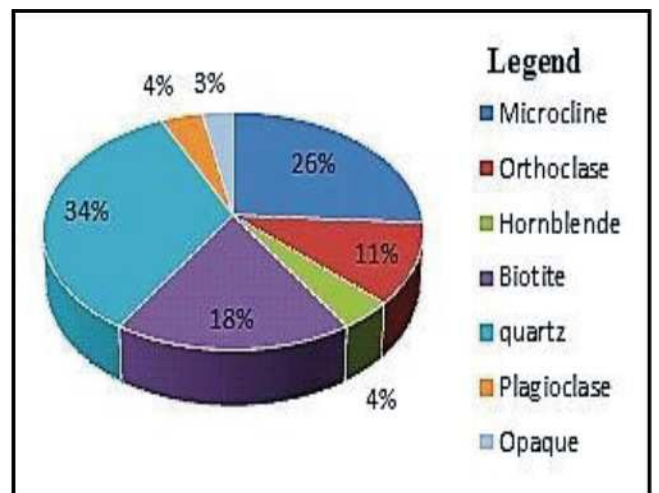


Fig. 9b: Modal composition of coarse under cross porphyritic granite

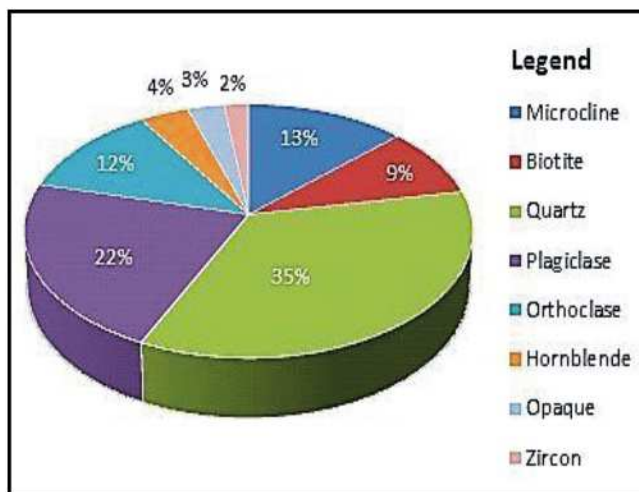


Fig. 8b: Modal composition of medium granite

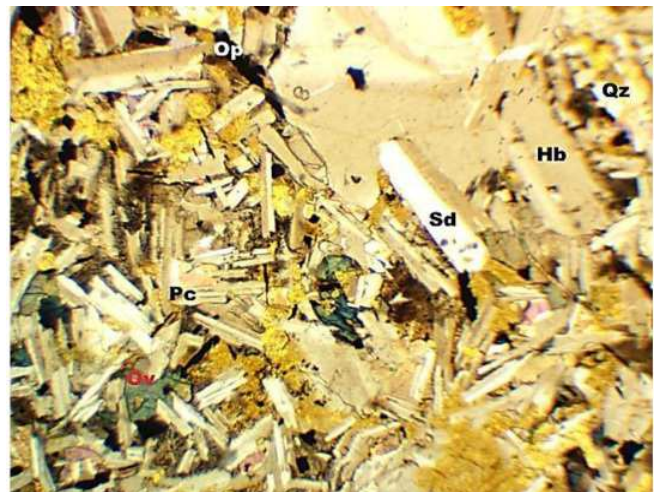


Fig. 10a: Photomicrograph of basalt under cross Figure

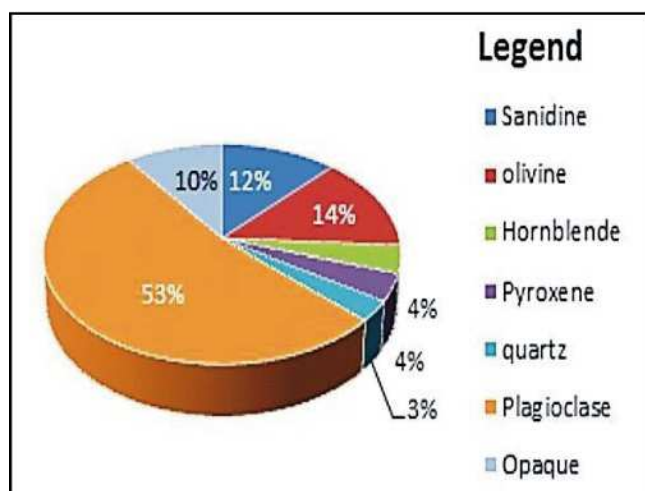


Fig. 10b: Modal composition of basalt polar (x20)

(Note: *Mc* – Microcline; *Pl*– Plagioclase; *Hb* – Hornblende; *Qz* – Quartz; *Sd* – Sanidine; *Ov* – Olivine; *Px* – Pyroxene; *Op*– Opaque; *Bt* – Biotite; *Oc* – Orthoclase, *Sp* – Sphene and *Zr* – Zircon)

medium grained granite (MGG), coarse grained granite (CGG), coarse porphyritic granite (OPG), basalt (BT) and pegmatite (PG).

Discussion

Lithologic Units

Migmatite-gneiss is medium grained, moderately foliated and consists of feldspar, biotite and quartz as dominant minerals. It occurs mostly as low-lying outcrops at the base of the granitic rocks in Holma, Hong and Fadama Rake areas (Figure 2). Granite gneiss is mesocratic, medium-coarse grained, mostly weakly foliated marked by alignment of mafic and felsic minerals along a preferred direction. It occurs mostly as pockets of low-lying outcrop at Mutaku hills and Fachi areas. The Older granite occurs as plutons dominated by boulders of different sizes and shapes covering more than a quarter of the study area. The medium grained granite is leucocratic and consists of quartz, feldspars and mica as dominant minerals (Figure 3). Coarse grained granite occurs at the base of the porphyritic granite and is also dominated by quartz, feldspars and biotite. The coarse porphyritic granite is dominated by large phenocryst of pink feldspars (microcline) with quartz and mica as subordinate minerals (Figure 4). Pegmatite and aplite occurs as tabular dyke-like intrusion containing mainly quartz and feldspar with subordinate mica. Basalts are fine to medium grained and occur both as massive bodies and boulders of different sizes and shapes (Figure 5). Most of the rocks have experienced some tectonic deformations

evidenced by the presence of joints, shear zones and faults. The gneisses, granites and the basalts have gradational as well as transitional boundaries while pegmatite and aplite have sharp boundaries with the country rocks.

Petrography

The mineral modes in migmatite-gneiss are hornblende, plagioclase, orthoclase, biotite, zircon, pyroxene, opaque and dominated by quartz (Figures 7A and 7B). Biotite, hornblende, opaque and plagioclase show parallel alignment along a preferred direction. The Older granite exhibits absences of alternating bands of micas and feldspars along a preferred direction. It is dominated by interlocking grains of quartz and feldspars minerals with subordinate biotite, muscovite and hornblende randomly disseminated within the groundmass. However, the mineral modes in medium grained granite are muscovite, hornblende, plagioclase, orthoclase, microcline, biotite, zircon, opaque and dominated by quartz (Figures 8A and 8B). Coarse porphyritic granite which is dominated by microcline feldspar also consists of muscovite, hornblende, plagioclase, orthoclase, quartz, biotite, sphene and opaque minerals (Figures 9A and 9B). The mineral assemblages in basalt which is dominated by plagioclase include, sanidine, pyroxene, quartz, olivine, hornblende and opaque (Figures 10A and 10B).

Plagioclase feldspar shows irregular grains, albite twinning while Orthoclase is anhedral- subhedral, cloudy, creamy-yellow to flesh pink, some unclear directional cleavages, low relief and not pleochroic. Microcline exhibits grid twinning (cross-hatched), colourless, cloudy and is massive with perfect cleavage that lacks pleochroism but shows first-order birefringence of white colour. The typical microcline clast in Figure 9A indicates feldspar porphyry. Quartz has anhedral to subhedral grains, poor relief, undulose/wavy extinction with creamy to colourless first-order interference colours and lacks twinning and visible cleavage while biotite is dark to brownish, strongly pleochroic and goes into parallel extinction. Hornblende is poikiloblastic, elongate in form and has strong pleochroism from brown to greenish-brown and goes into inclined/oblique extinction at an angle of 20°. Pyroxene is prismatic with good directional cleavage that meets at obtuse angle. Zircon is pleochroic, prismatic with bipyramid terminations displaying knee-shaped twins showing high relief with moderate birefringence of first to second- order of bluish colour. Sanidine feldspars show prismatic tabular/lath shapes

Table 1: Geochemical Results

Major Oxides																		
RKS/ Oxide	MG 1	MG 2	MG 3	GG 1	GG 2	MGG 1	MGG 2	CGG 1	CGG 2	OPG 1	OPG 2	OPG 3	BT1	BT 2	BT 3	PG 1	PG 2	PG 3
SiO ₂	67.3	67.52	66.2	68.43	68.88	70.66	70.50	69.04	71.02	69.27	68.34	67.88	47.76	46.65	45.87	64.45	65.30	65.77
Al ₂ O ₃	12.4	11.5	13.2	11.9	11.5	14.3	14.7	15.3	14.2	12.9	12.0	11.6	16.1	16.7	17.1	17.5	17.1	16.6
SO ₃	<0.04	<0.04	<0.04	<0.2	<0.2	0.1	0.1	0.1	0.1	0.1	0.1	0.1	<0.1	<0.1	<0.1	<0.1	<0.1	<0.1
P ₂ O ₅	0.04	0.04	0.05	0.05	0.06	0.07	0.06	0.08	0.07	0.08	0.06	0.09	0.09	0.08	0.1	0.29	0.56	0.34
Fe ₂ O ₃	5.98	6.63	5.89	4.92	4.77	6.64	5.06	4.64	5.52	6.00	5.53	5.67	14.1	15.0	15.5	0.97	1.49	2.07
TiO ₂	1.34	1.44	1.40	1.10	1.03	1.10	1.20	1.23	1.21	1.28	1.31	1.35	4.35	4.01	3.27	0.06	0.08	0.12
MgO	1.53	1.76	1.50	1.72	1.68	1.30	1.10	1.40	1.60	1.80	1.90	1.70	6.49	6.78	5.99	0.02	0.06	0.04
CaO	3.11	3.01	2.54	2.96	3.07	1.45	1.38	1.42	1.39	1.41	1.43	1.50	7.56	7.11	7.64	0.40	0.43	0.76
Na ₂ O	1.87	1.96	2.0	3.99	4.00	3.00	2.05	3.20	2.18	3.00	3.31	4.00	2.23	2.08	2.12	2.60	3.00	2.84
K ₂ O	3.20	3.78	3.54	3.35	3.75	3.75	3.50	3.83	3.57	4.00	4.16	4.40	1.55	1.45	1.77	11.4	10.8	9.98
BaO	0.72	0.91	0.54	0.66	0.56	0.46	0.36	0.64	0.25	0.62	0.90	1.00	0.97	0.89	1.06	0.81	0.90	1.00
LOI	0.55	0.51	0.55	0.47	0.45	0.40	0.44	0.43	0.40	0.44	0.43	0.41	0.40	0.40	0.40	0.50	0.51	0.51
Total	99.39	100.21	100.11	99.66	99.71	101.70	100.44	101.26	101.53	100.90	99.47	100.05	101.61	101.17	100.78	99.07	100.22	100.14
Trace Elements																		
Hf	0.5	0.7	0.3	0.80	0.68	1.43	1.56	0.8	0.97	1.12	1.05	1.20	13.5	11.4	12.5	36.1	42.0	52.2
Li	20.5	15.8	18.5	15.9	16.8	80.3	87.3	23.6	25.1	39.7	38.0	37.8	40.2	42.1	41.3	-	-	-
Rb	80.5	85.7	95.4	158	171	211	201	170	170	220	200	200	38.7	40.3	46.8	665	710	816
Ta	1.2	0.8	1.0	0.97	1.10	2.81	2.69	1.10	0.95	1.04	0.95	0.89	7.70	6.8	7.40	64.3	77.1	83.2
Nb	26.9	24.3	23.9	12.8	10.9	30.7	28.8	12.3	10.8	15.0	14.7	14.0	70.0	66.8	68.6	-	-	-
Cs	1.8	2.0	1.7	1.4	1.36	7.70	8.0	2.06	2.12	6.50	6.20	6.43	0.71	0.56	0.65	16.5	18.3	20.0
Ba	200	195	181	137	146	689	658	653	672	965	951	958	365	355	360	130	148	154
Co	16	17	16	13	11	12	15	14	16	19	21	19	51	49	57	<1	<1	<1
Pb	6.4	5.9	5.7	35.1	31.8	35.2	37.8	21.3	22.7	20.2	19.7	18.9	7.50	7.3	7.00	-	-	-
Sc	12	11	15	7	9	3	2	3	5	4	1	2	-	-	-	3	6	4
Zn	20.2	22.8	20.5	107	113	329	333	253	233	281	288	289	203	200	201	52.9	53.0	58.0
Sr	112.0	125.7	115	104	115	237.0	346	342	287	478	545	650	299	345	385	5.0	6.1	6.9
Zr	20.5	22.2	19.7	18.5	20.5	22.7	23.6	13.8	15.1	29.4	28.7	30.0	453	459	451	-	-	-
Th	4.12	4.09	4.89	8.34	9.0	9.30	9.7	7.9	7.5	5.21	4.87	5.0	5.00	5.2	4.9	180	167	155
U	2.01	1.91	1.87	1.80	1.98	2.40	2.37	1.5	1.3	1.89	1.97	1.90	1.30	1.53	1.44	12.4	18.6	16.2
Tl	0.20	0.1	0.2	0.82	0.67	1.70	1.9	1.03	0.98	0.51	0.52	0.50	0.35	0.32	0.33	-	-	-
Mn	394.7	400.4	387.3	257	268	1161	1175	1065	1108	929	976	944	2476	2455	247	-	-	-
Ho	1	1.2	1.4	1.8	2	1	1.7	2.2	1.9	0.9	0.7	0.5	1.2	0.9	0.6	<0.1	<0.1	<0.1
Gd	7.5	7.3	8	5.7	4.9	5.2	6.1	8.4	9.5	5.7	4.2	6.9	5.3	4.8	6.4	9.1	0.3	0.4
V	54	46	62	13	18	6	5	2	5	9	8	10	176	188	161	-	-	-
Cu	<10	<10	<10	<10	<10	<10	<10	<10	<10	<10	<10	<10	47	50	52	<10	<10	<10
Sn	4	3	4	3	3	4	3	5	7	4	4	6	15.8	13.7	9.6	7	15	10
Ni	<20	<20	<20	<20	<20	<20	<20	<20	<20	<20	<20	<20	176	162	193	<20	<20	<20
Ga	37	28	27	24	25	19	22	21	13	25	29	36	17	19	18	-	-	-
REE																		
Dy	1.76	1.98	1.66	1.71	1.82	2.4	2.2	1.50	1.43	1.44	1.43	1.36	5.80	4.90	5.5	0.50	0.4	0.62
Lu	0.03	0.03	0.04	0.03	0.03	0.10	0.12	0.1	0.1	0.21	0.23	0.20	-	-	-	0.10	0.10	0.10
Nd	45.73	43.3	50.9	37	40	36	48	82	90	95	102	120	33.0	32.1	33.4	27.3	25.2	24.8
Yb	0.32	0.33	0.40	0.28	0.23	0.95	1.0	1.1	1.2	1.42	1.50	1.40	1.20	1.2	1.21	6.10	7.12	8.08
Y	37	30	26	48	52	20	37	45	53	39	33	28	19.4	20.5	21.2	<2	<2	<2
Ce	43.7	45.7	44.8	52.9	55.6	19.76	20.45	45.7	43.8	77.6	76.4	77.0	101	97.8	100	67.8	76.8	88.2
La	16.7	17.2	16.4	65.4	64.7	13.3	15.0	6.99	7.12	44.8	43.1	43.8	20.1	19.7	19.5	21.5	25.6	27.0
Pr	0.94	1.1	0.60	1.50	1.60	2.41	2.76	1.61	1.70	12.3	11.6	11.1	4.40	4.3	4.3	0.23	0.30	0.4
Sm	1.28	1.45	1.05	2.83	3.05	3.40	3.90	4.20	4.0	7.0	6.50	7.34	4.87	3.57	4.67	1.47	2.06	2.44
Eu	0.086	0.076	0.059	0.08	0.08	0.23	0.32	0.44	0.45	1.02	0.9	0.9	0.30	0.30	0.31	0.30	0.10	0.21

showing simple twin (Carlsbad) with two perfect cleavages. Olivine is pale-green to brownish, hexagonal or spindle shaped. Opaque minerals are few and anhedral in shape.

Geochemistry

Geochemical results in Table 1 and Figures 11-13

revealed that granite gneiss and the Older granite are enriched in SiO₂ with ranges from 67.8 to 71.02 wt. %, K₂O (3.35 - 4.40 wt. %) and Na₂O (2.18 - 4.00 wt. %) but depleted in Fe₂O₃, Al₂O₃ and TiO₂. Migmatite-gneiss is also enriched in SiO₂ with ranges from 62.20 - 67.52 wt. % but depleted in Na₂O with ranges from 1.87- 2.00 wt. % relative to enrichment in granite. Expectably, basalts are enriched in MgO with ranges from 5.99 - 6.78 wt. %,

TiO₂ (3.27 - 4.35 wt. %), Fe₂O₃ (14.1 - 15.5 wt. %) and CaO (7.11 - 7.64 wt. %). Pegmatite is enriched in Al₂O₃ (16.6 - 17.5 wt. %) and K₂O (9.98 - 11.4 wt. %), relatively enriched in SiO₂ (64.45 - 65.44 wt. %) but depleted in CaO, (0.40 - 0.76 wt. %), Fe₂O₃ (0.87 - 2.07 wt. %) and TiO₂ (0.06 - 0.12 wt. %). The enrichment of SiO₂ and depletion in Al₂O₃ in the gneisses and the Older granite depicts acidity which is attributed to abundance of quartz as revealed by petrography of the rock. The enrichment of Fe₂O₃ and TiO₂ in the basalt denotes basicity which is attributed to abundance of plagioclase feldspars and opaque which is consistent with petrographic studies. The enrichment of K₂O, CaO, and Na₂O in granites and pegmatite depicts alkalinity which is attributed to abundant occurrence of K-feldspars as shown by the modal compositions of the rocks. The depletion in the concentration of Fe₂O₃ and CaO, the enrichment in SiO₂ and Na₂O and the close similarities of the values in granite gneiss with the granites may be evidence of crystallization and evolution of the granite gneiss from felsic parent rock probably the Older granite.

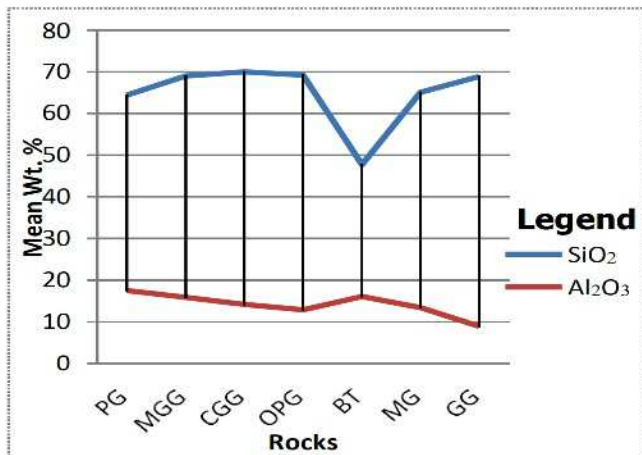


Fig. 11: Variation plot of SiO₂ and Al₂O₃

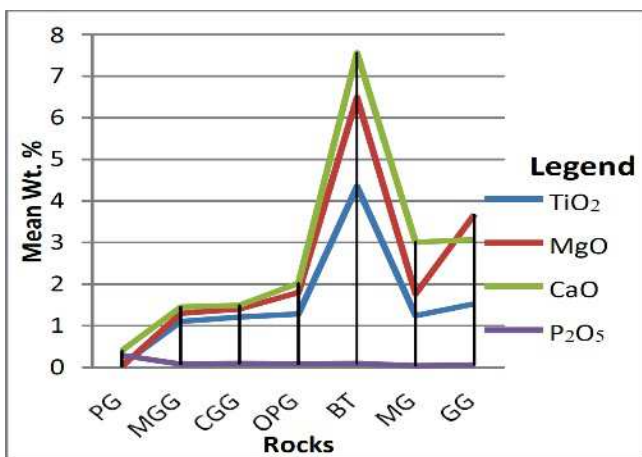


Fig. 12: Variation plot of TiO₂, MgO, CaO and P₂O₅

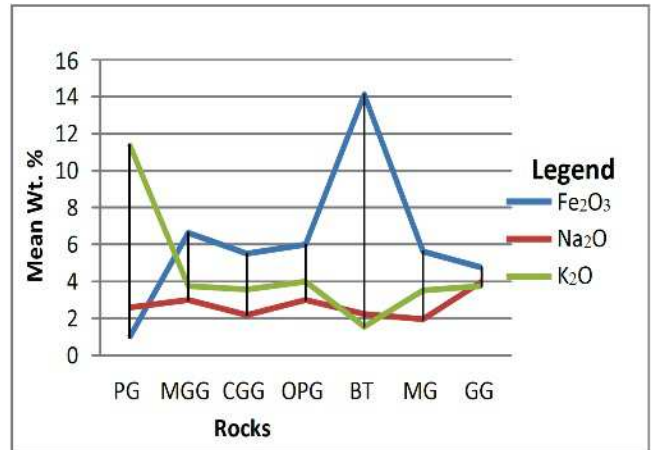


Fig. 13: Variation plot of Fe₂O₃, Na₂O and K₂O

Some selected oxides and trace elements plotted on Harker using SiO₂ as fractionation index for gneisses, granites and pegmatite and MgO as fractionation index for basalts shows that major oxides of Fe₂O₃, CaO and Al₂O₃ and MgO vs. K₂O shows continuous negatively correlated well-defined linear trend for gneisses, granites, pegmatite and basalt respectively (Figures 14 - 17). Similarly, Harker plots of SiO₂ against some selected trace elements (Co and Sr) equally show well-defined negative linear trend (Figures 18 - 19). Lithophile element of Rb plotted against Sr on Harker also show a negative well-defined linear trend (Figure 20). The continuous negative correlated well-defined linear trend in gneisses and granites suggest that Fe₂O₃, CaO, Al₂O₃, Co, and Sr abundances decreases with increase in SiO₂. Similarly, MgO increases with decrease in K₂O in the basalts. These negative well-defined linear trend correlations of the various rocks on the Harker plot suggest fractionation of the magma and the falling of some of the rocks on the same linear line suggest that these rocks are co-magmatic (Zorano *et al.*, 2007, Maulana *et al.*, 2012).

The enrichment in the large ion lithophile elements (LILE) of Th, U, Ba, Pb, K, Sr Rb and Ce in gneisses and granites and Rb, Th, Hf, Zr and Nb in pegmatite (Table 1) and their corresponding positive anomalies on the chondrite normalized spider plots (Figures 21 - 26) indicates calc-alkaline and crustal affinity. On the other hand, the enrichment of Co, Cs, Mn, Ni, Pb and Ta (Table 1) in basalt and their corresponding positive anomalies on the chondrite normalized spider plots (Figure 27) suggests basicity of the rock and mantle affinity. The enrichment in the high field strength elements (HFSE) of Zr, Hf, Nb, Ta and Th and the variations in the values of Ba with respect to Sr and Rb in the rocks indicate fractionation (Zorano *et al.*, 2007,

Ugwuonah, 2009 and Ugwuonah and Obiora 2011).

The chondrite-normalized REE patterns of the rocks in the study area are characterized by enrichment in LREE relative to depletion in HREE (Figure 21 - 26). According to Compton (1978), the enrichment in LREE and depletion in HREE suggest that the melts from which these rocks were formed equilibrated with residual garnet (which is the principal reservoir of HREE) and may also contain high concentration of Zircon, apatite (which is also responsible for HREE retention). This demonstrates calc-alkaline/basicity of the rocks. The prominence of negative values of Eu in all the rocks and with regards to their relationship with plagioclase and K- feldspars and its removal during partial melting shows a highly fractionated magma source since feldspars are the only rock forming minerals which are relatively enriched by Eu (Girei 2015).

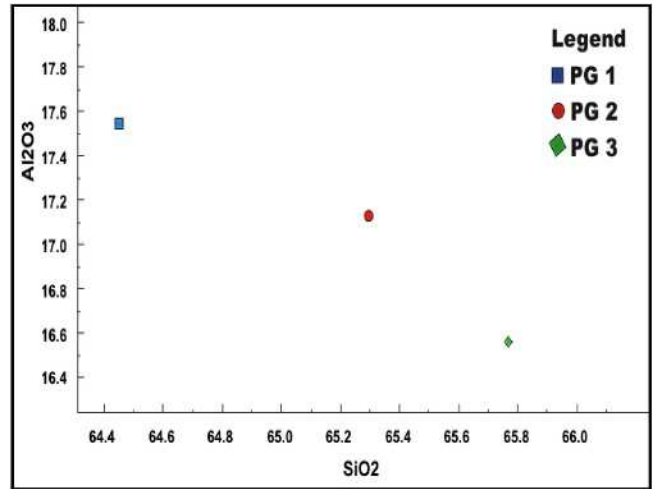


Fig. 16: Harker plot of SiO₂ vs. Al₂O₃ for basalt

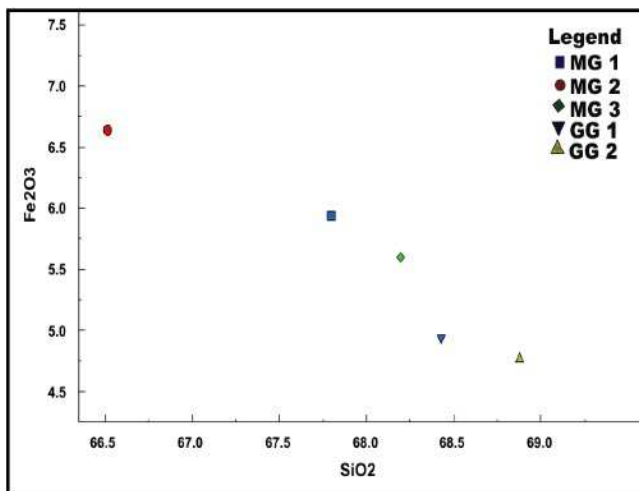


Fig. 14: Harker plot of SiO₂ vs. Fe₂O₃ for gneisses

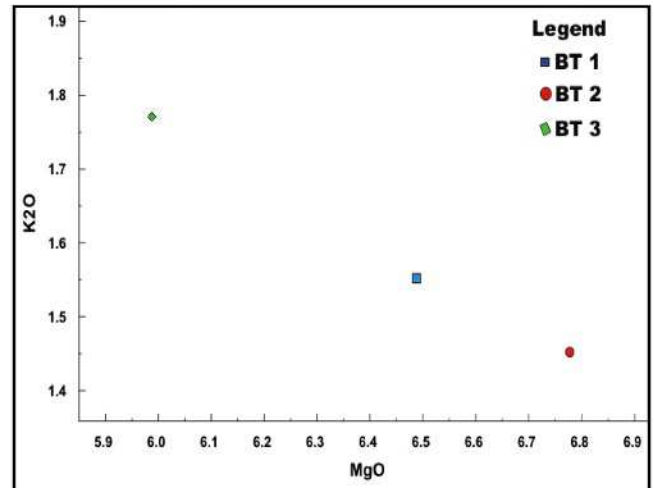


Fig. 17: Harker plot of MgO vs. K₂O pegmatite

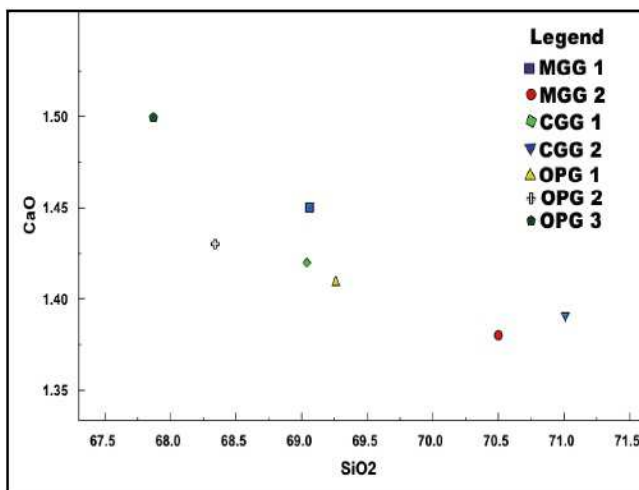


Fig. 15: Harker plot of SiO₂ vs. CaO for Granite

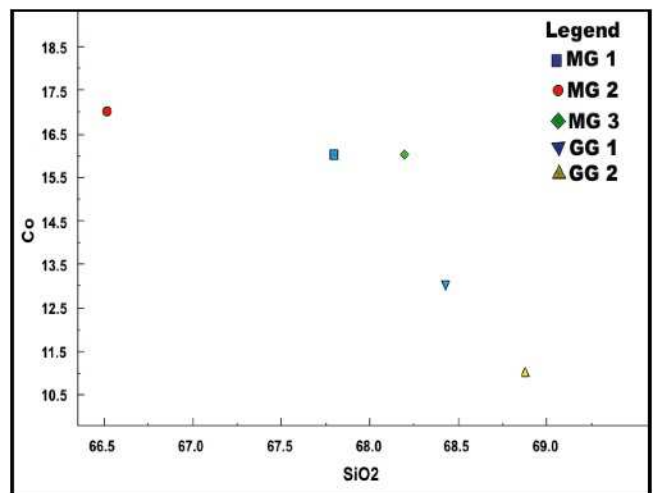


Fig. 18: Harker plot of SiO₂ vs. Co for Granites

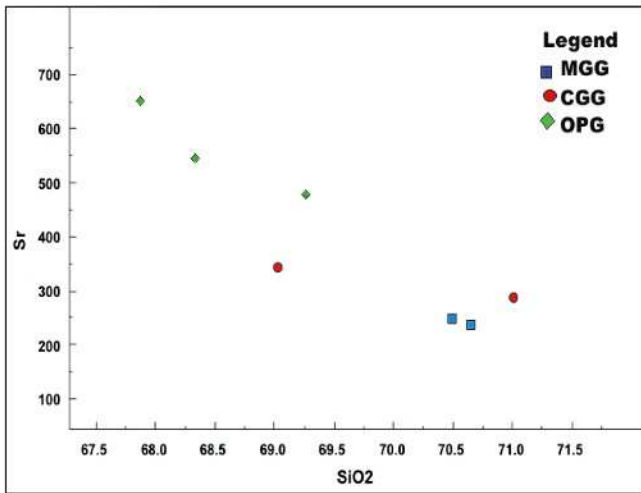


Fig. 19: Harker plot of SiO₂ vs. Sr for Granites

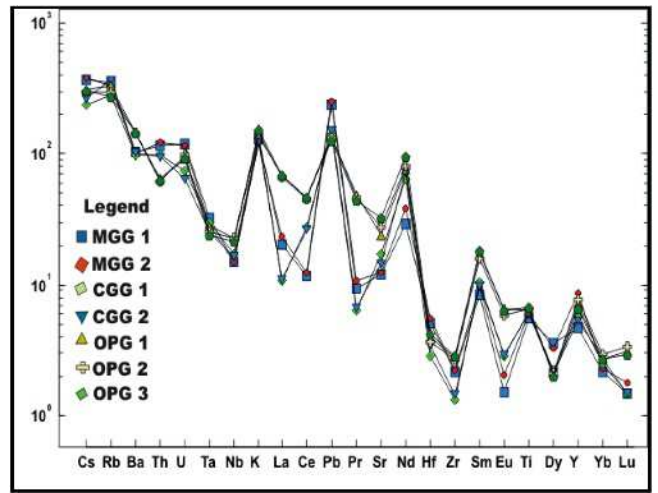


Fig. 22: Chondrite normalized spider plot for granites after McDonough and Sun (1995)

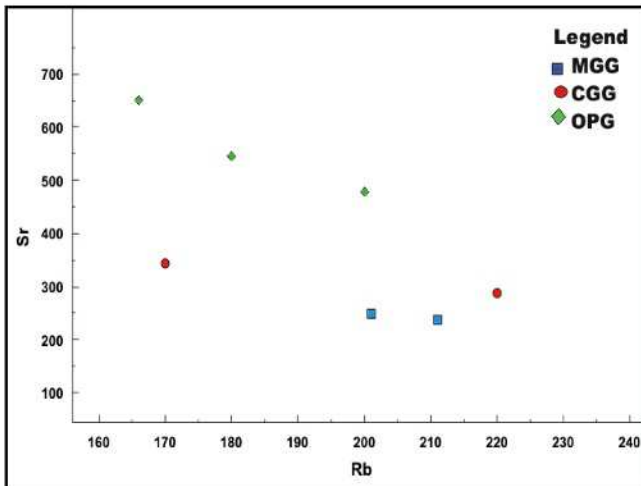


Fig. 20: Plot of Rb vs. Sr for Granite

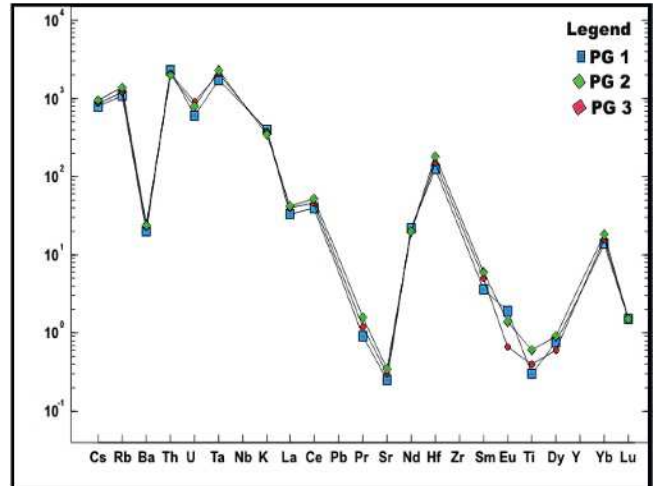


Fig. 23: Chondrite normalized spider plot for pegmatite after McDonough and Sun (1995)

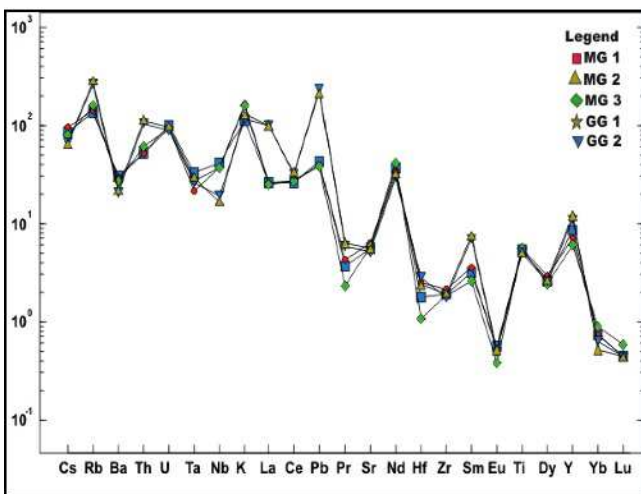


Fig. 21: Chondrite normalized spider plot for gneisses after McDonough and Sun (1995)

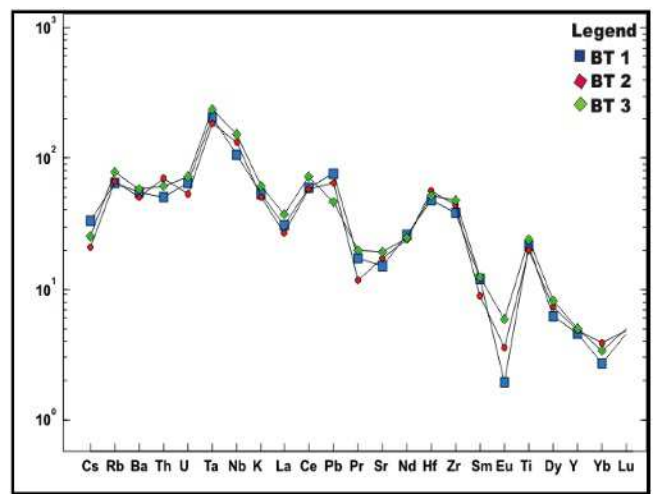


Fig. 24: Chondrite normalized spider plot for basalt after McDonough and Sun (1995)

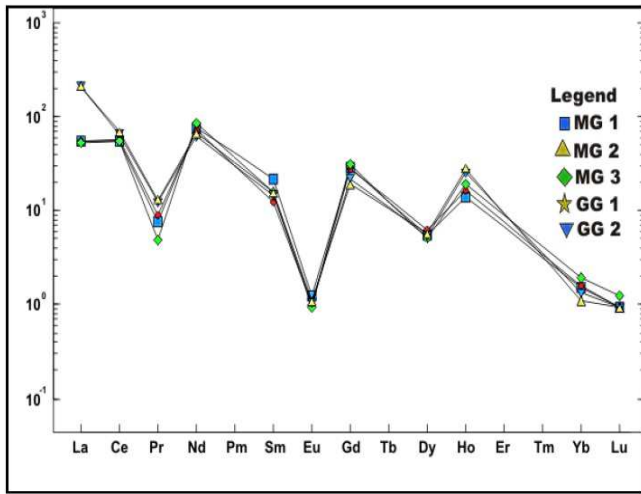


Fig. 25: Chondrite normalized spider plot for gneisses after Boynton (1984)

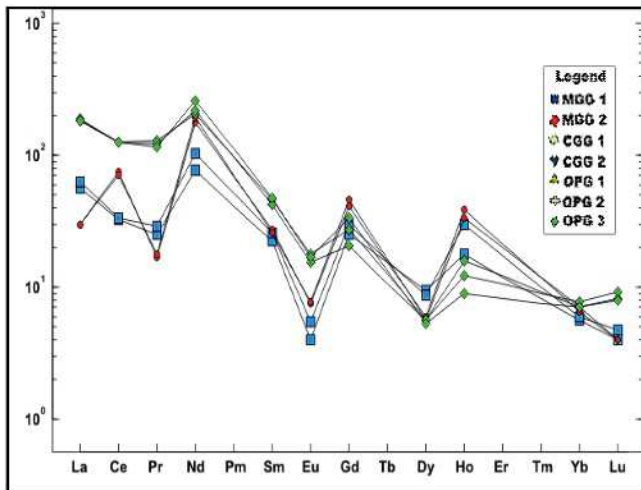


Fig. 26: Chondrite normalized spider plot for granite after McDonough and Sun (1995)

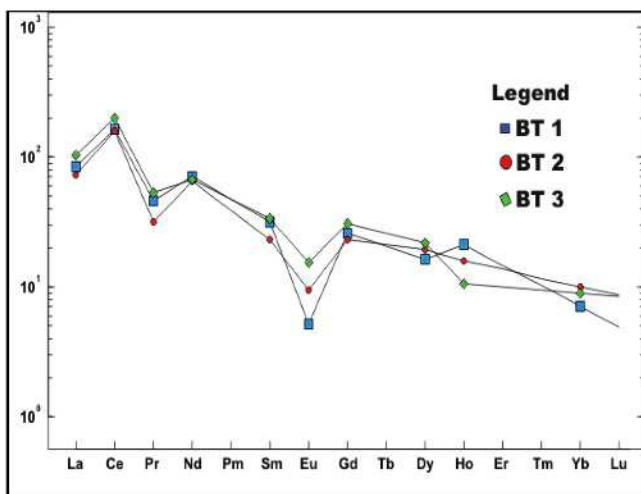


Fig. 27: Chondrite normalized spider plot for basalt after Boynton (1994)

General Classification

Tectonic discrimination diagrams of Rb vs. (Yb + Ta) after Pearce et al (1984) shows that granite gneiss and granites are sandwiched between volcanic arc granite (VAG) and Syn-COLG (Figure 28). Discrimination diagram of Zr-Ti-Sr after Pearce and Cann (1973) for basalts in Figure 29 shows that the basalts are mid oceanic ridge (MORB). TAS discrimination diagrams of SiO₂ vs. Na₂O + K₂O after Cox-Bell-Pank (1979) shows that granite gneiss and granites fall within the granite field (Figures 30 and 31). This has further confirmed the evolution of the granite gneiss from the Older granite. Discrimination plot of SiO₂ against Na₂O + K₂O after Le Bas (1986) for basalt shows basalt plotting within the basalt field (Figure 32). On the other hand, AFM diagrams after Irvine and Baragar (1971) shows that the gneisses, granites and pegmatite are calc-alkaline while basalt is tholeiitic (Figure 33). Discrimination diagrams of K₂O vs. Na₂O after Rajesh and Santosh (2004) shows that the granites are I-type (Figure 34), metaluminous to weakly peraluminous (Chappell *et al.* 2012) and are characterized by the presences of hornblende which are derived due to partial melting of igneous protolith (Clemens and Stevens, 2012).

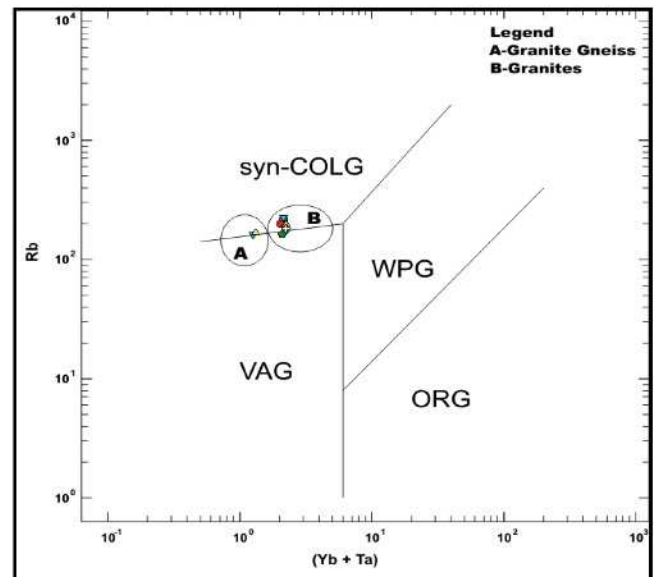


Fig. 28: Discrimination Diagram of Rb (Yb+Ta) for granite gneiss and granitoids after Pearce *et al.* (1984)

Petrogenesis

The negative distribution trend of Ta, Nb, Sr and Eu; the enrichment of Rb, Ba, Sr K, U and Th in gneisses, granites and pegmatite and the calc-alkaline affinity is typically associated with magmas evolved from

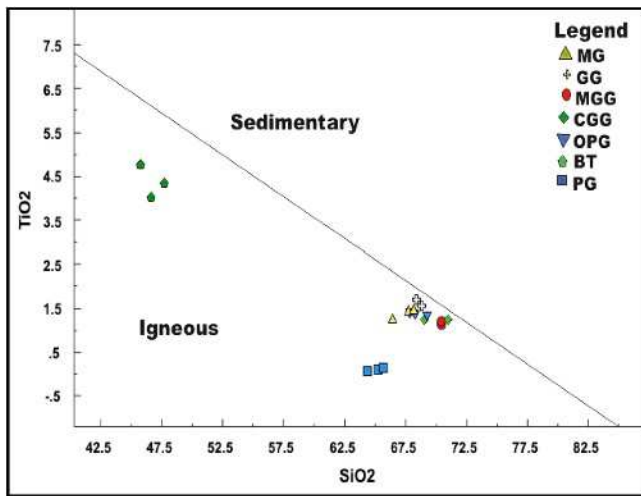


Fig. 35: Discrimination diagram of SiO₂ vs. TiO₂ after Rajesh and Santosh (2004)

continental crust (Ugwuonah, 2009; Ugwuonah and Obiora, 2011). The enrichment in LREE relative to depletion in HREE in the granite gneiss and granite suggests that their progenitors were derived from a cratonic source because the principal carriers of REEs in most granite are the accessory minerals such as monazite, zircon and apatite (Ugwuonah, 2009 and Ugwuonah and Obiora, 2011). Saleh and El-Nisr, (2013) further stated that fractionation of such accessory minerals results in lowering of REEs content in the granites. On the other hand, the enrichment of Ni, Ti and Fe₂O₃ is attributed to the abundance of olivine, pyroxene and opaque (Fe₂O₃) in basalt and suggest mantle source (Brophy, 2008). The LREE depletion in basalt reflects the incompatible element-depleted nature of the upper mantle from which these magmas were

derived. The negative linear trend correlations and the negative Eu of the rocks suggest that the rocks most likely resulted from fractional crystallization during magmatic evolution (Maulana *et al.*, 2012). Discrimination diagram of SiO₂ vs. TiO₂ after Rajesh and Santosh (2004) revealed that all the rocks in the study area suggest igneous progenitors (Figure 35).

Conclusions and Recommendations

Field, petrography and petrochemical data has differentiated the rocks of Pella into migmatite-gneiss, granite gneiss, basalt and pegmatite. The petrographic results have agreed with geochemical data and ground truthing. The geochemical data have also proven that the major rocks in Pella are dominantly calc-alkaline, fractionated and have continental crust affinity. The similarities in data of the granite gneiss and granites show that they are genetically related to a common source. Unless otherwise proven, anatexis is responsible for the evolution of the rocks in Pella and environs. On the other hand, it is strongly recommended that further studies be carried out in adjoining areas to further unravel the geology of the area with the view of differentiating the rocks.

Acknowledgements

The assistance given by Mr. and Mrs. Unachukwu is acknowledged. I also appreciate the support and guidance of Prof. N. E. Bassey who was in the field with me. Finally, the encouragement of Dr. Abdulrazaq Garba (DG, Nigerian Geological Survey Agency) is highly appreciated.

References

- Adekeye, J.L.D and Ntekim, E.E. (2004): The Geology of Song area in Southern Hawal Massif, N.E. Nigeria. *Zuma Journal of Pure and Applied Sciences* 6 (2), pp 145 – 151.
- Bassey, N. E. (2006). *Structural geological mapping and interpretation of landsat and aeromagnetic data over parts of Hawal Basement complex, N.E. Nigeria*. Ph.D thesis (unpublished) Abubakar Tafawa Balewa University, Bauchi Pp. 218.
- Bassey, N. E. and Valdon, Y.B. (2011): Structural Features and Rock Crystal Mineralization in Dumne Area, Hawal Basement Complex, N.E. Nigeria. *International Journal of Environmental Science*, vol. 7, No. 3. pp 1 – 8.
- Boynton W. V. (1984) Cosmochemistry of the REE Meteorite Studies in REE Geochemistry, Henderson P (Editor), Elsevier Science Publ. Co. Amsterdam.
- Brophy, J.G. (2008). A study of rare earth element (REE)–SiO₂ variations in felsic liquids generated by basalt fractionation and amphibolite melting: a potential test for discriminating between the two different processes. *Contrib Mineral Petrol*
- Chappell B.W., Bryant C.J., and Wyborn D., (2012): Peraluminous I-type granites. *Lithos* 153: pp. 142–153
- Clemens, J.D., and Stevens, G., (2012). What controls chemical variation in granitic magmas. *Lithos*, 134: pp. 317–329

- Compton, P. (1978): Rare earth evidence for the origin of the Nuk Gneisses Buksefjorden Region South west Greenland. *Contribution to mineral and Petrology*, 66: pp. 283-293.
- Cox KJ, Bell JD, Pankhurst RJ (1979) The interpretation of igneous rocks. George Allen and Unwin Ltd, London, p450.
- Federal Surveys (1968): Topographic map of Shellen, sheet 175. Published by Directorate of Overseas Survey for Nigerian Government.
- Girei, B.M (2015). Geology, Geochemistry and Petrogenesis of granite suites and pegmatites in the northern part of Mandara hills Gwoza sheet 114, northeastern Nigeria. A Thesis submitted to the School of Postgraduate Studies, Ahmadu Bello University, Zaria in partial fulfillment of the requirements for the award of a Master Degree in Geology. Unpublished. 160 Pp.
- Irvine, T.N. and Baragar, W.R.A., 1971. A guide to the chemical classification of the common volcanic rocks. *Can. J. Earth Sci.* 8, 523-548.
- Kwache, J.B and Ntekim, E.E (2015). The Geology of Dumne Area in Southern Hawal Massif Northeastern Nigeria. *International journal of Science and Research, Volume 4 Issue 11*, pp 2477-2482.
- Le Bas MJ, Le Maitre RW, Streckeisen A, Zanettin B. (1986) A chemical classification of volcanic rocks based on the total alkali-silica diagram. *J Petrol* 27: 745-50
- Maulana A., Watanabe K., Imai A., Yonezu K., (2012): Petrology and Geochemistry of Granitic Rocks in South Sulawesi, Indonesia: Implication for Origin of Magma and Geodynamic Setting. *International Journal of Environmental, Earth Science and Engineering* 6 (1): pp. 1-6
- McCurry P, (1976) A General Review of The Geology of the Precambrian to Lower Palaeozoic Rocks of Northern Nigeria in *Geology of Nigeria* Edited by C. A. Kogbe published by Rock View (Nigeria) Limited, Plot 1234 Zaramaganda, Yakubu Gowon Way, Jos
- McDonough, W. F and Sun, S.S (1995) Primitive Mantle In: WinRock software developed by Rob Kanen (2004) Published by MinSer
- Patrick, J.O. (2005): *Geological Mapping of Parts of Song Area, Adamawa State, Northeastern Nigeria*. B.Tech. Thesis, Department of Geology, Federal University of Technology, Yola. Unpublished. 67p.
- Pearce, J.A and Cann, J.R., 1973. Tectonic setting of basic volcanic rocks determined using trace element analyses. *Earth and Planetary Science Letters* 19, 290-300.
- Pearce J.A., Harris N.B and Tindle A.G. (1984): Trace element discrimination diagrams for the tectonic interpretation of granitic rocks. *Journal of Petrology*. 25: pp. 956–983
- Rajesh H.M and Santosh M 2004. Charnokitic Magmatism in southern India. *Proc. Indian Acad. Sci. (Earth and Planetary Science)*, 113 No. 4, pp. 565-585
- Saleh G. M. and El-Nisr S.A. (2013): Two Mica Granites, Southeastern Desert, Egypt: Geochemistry and Spectrometric Prospecting. *Greener Journal of Geology and Earth Sciences* 1(2): pp. 23-42
- Ugwuonah, C.N (2009). *Petrology and Geochemistry of the Basement Complex Rocks Around Keffi Northcentral Nigeria*. An M.Sc. Thesis submitted to Geology Department, University of Nigeria, Nsukka. 79p. Unpublished.
- Ugwuonah, E.N and Obiora, S.C., (2011). Geothermometric and Geobarometric Signatures of metamorphism in the Precambrian Basement Complex Rocks around keffi, Northcentral Nigeria. *Ghana Journal of Science*, 51, 73–87.
- Zorano S.S; Martin H., Jean-Jacques P; Emanuel F.J and Maria H.F.M (2007): Calc-Alkaline Magmatism at the Archean-Proterozoic Transition: the Caico Basement Complex (NE Brazil) *Journal of Petrology* 48 (11): pp. 2149-2185
-



GARNET ENERGY SERVICES NIGERIA LTD.

Geological, Petroleum and Environmental Consultants

12 Floor, Bookshop House, 50/52 Broad Street, Lagos
 P.O. Box 70011, Victoria Island, Lagos, Nigeria
 Tel. 01-8546699, 06035101804
 E-mail mariesonuga@yahoo.com



BARACAL CONSULT LTD.

Environmental Consultants

Suite 65/66 Dolphin Plaza, Dolphin Estate, Ikoyi
 P.O. Box 70885, Victoria Island, Lagos, Nigeria
 Tel. 234-1-7741441, 234-1-2629251 Fax 234-1-2610735
 E-mail baracalnig@yahoo.com, carolsoladg@yahoo.com



Jonakod Nigeria Limited

Energy, Environment & Safety Consultants

34 Ontario Crescent, Maitama, Abuja
 Tel. 09-4133521, 08035300958, 08057467878
 E-mail jonas_odocha@yahoo.com



AMJU SERVICES NIG. LTD.

Specialists in Geological & Mining Services

1B Rock Road, Off Rabah Road
 P.O. Box 7216, Kaduna, Nigeria
 Tel. +234-(0)8054073338
 E-mail abuykarofi@gmail.com
